

Amplification of polarization NOON states

Chiara Vitelli¹, Nicolò Spagnolo¹, Fabio Sciarrino^{2,1}, and Francesco De Martini^{1,3}

¹Dipartimento di Fisica dell'Università "La Sapienza" and Consorzio Nazionale Interuniversitario per le Scienze Fisiche della Materia, Roma 00185, Italy

²Centro di Studi e Ricerche "Enrico Fermi", Via Panisperna 89/A, Compendio del Viminale, Roma 00184, Italy

³Accademia Nazionale dei Lincei, Italy

NOON states are path entangled states which can be exploited to enhance phase resolution in interferometric measurements. In the present paper we analyze the quantum states obtained by optical parametric amplification of polarization NOON states. First we study, theoretically and experimentally, the amplification of a 2-photon state by a collinear Quantum Injected Optical Parametric Amplifier (QIOPA). We compared the stimulated emission regime with the spontaneous one, studied by Sciarrino et al. (PRA **77**, 012324), finding comparable visibilities between the two cases but an enhancement of the signal in the stimulated case. As a second step, we show that the collinear amplifier cannot be successfully used for amplifying N-photon states with $N > 2$ due to the intrinsic $\frac{\lambda}{4}$ oscillation pattern of the crystal. To overcome this limitation, we propose to adopt a scheme for the amplification of a generic state based on a non-collinear QIOPA and we show that the state obtained by the amplification process preserves the $\frac{\lambda}{N}$ feature and exhibits a high resilience to losses. Furthermore, an asymptotic unity visibility can be obtained when correlation functions with sufficiently high order M are analyzed.

I. INTRODUCTION

In the last few years it has been proposed to exploit quantum effects to provide resolution enhancement in imaging procedures. Among the numerous problems that are currently studied under the general name of *quantum imaging*, the investigations concerning the quantum limits on optical resolution have a special importance, as they may lead to new concepts in microscopy and optical data storage. Such so-called *super-resolution* techniques, studied for a long time at the classical level in the perspective of beating the Rayleigh limit of resolution, were recently revisited at the quantum level [1]. It was shown that it was possible to improve the performance of super-resolution techniques by adopting non-classical light [2, 3]. This approach, *quantum lithography*, may lead in the future to innovative microscopy techniques, to record features in images which are much smaller than the wavelength of the light or to improve the optical storage capacity beyond the wavelength limit. In such framework, path entangled NOON states $|\psi^N\rangle_{AB} = \frac{1}{\sqrt{2}} (|N\rangle_A |0\rangle_B + |0\rangle_A |N\rangle_B)$ have been adopted to increase the resolution in quantum interferometry. Indeed in such states a single mode phase shift φ induces a relative shift between the two components equal to $N\varphi$. This feature leads to a sub-Rayleigh resolution scaling as $\frac{\lambda}{2N}$, λ being the wavelength of the field [4]. The theoretical and experimental study of photonic NOON states [5] has led to the experimental a posteriori generation of two, three and four photons states [6, 7, 8] and to the conditional generation of a state with $N = 2$ [9]. Furthermore, very recently schemes for the generation of path-entangled NOON states with high value of fidelity and arbitrary N have been proposed [10, 11]. However, the weak value of the generated number of photons strongly limits the potential applications to quan-

tum lithography and quantum metrology. Furthermore a NOON state, as any superposition of macroscopic states, is "supersensitive" to losses. Hence for a N-photon state a fractional loss $\frac{1}{N}$ would destroy the quantum effect responsible for the phase resolution improvement.

A natural approach to increase the number of photons and to minimize the effect of losses is to exploit the process of stimulated emission. This process, also known as quantum injected optical parametric amplification, has been first studied in [12], and has found some important applications in the context of quantum information [13, 14, 15]. Recently the output radiation of an unseeded optical parametric amplifier (OPA) has been exploited to show the typical $\lambda/4$ feature [16] Fig.1-(a). In the present paper we investigate the task of the amplification of photonic NOON states by two different devices, both based on a quantum injected optical parametric amplifier (QIOPA). First, in Sec.II, we review how a sub-Rayleigh $\frac{\lambda}{2N}$ resolution can be obtained by an interferometric device acting on a NOON state and we show how the performances of this scheme are affected by losses. Then, in Sec.III we study both theoretically and experimentally the amplification of a 2 photon state by a collinear QIOPA, as shown schematically in Fig.1-(b), investigating how the features of the state are modified when the entanglement is broadcasted via amplification over a large number of particles. An experimental comparison with the spontaneous field Fig.1-(a) of the collinear OPA, that intrinsically has a $\frac{\lambda}{4}$ feature [16], shows that the visibilities in the two regimes are comparable, while the injected case manifests an increase of the signal due to the stimulated emission process. We then show that this device cannot be successfully used to amplify a generic N-photon state since the typical $\frac{\lambda}{2N}$ feature of the seed is lost. Finally, in Sec.IV, we propose to exploit a non-collinear QIOPA in order to amplify

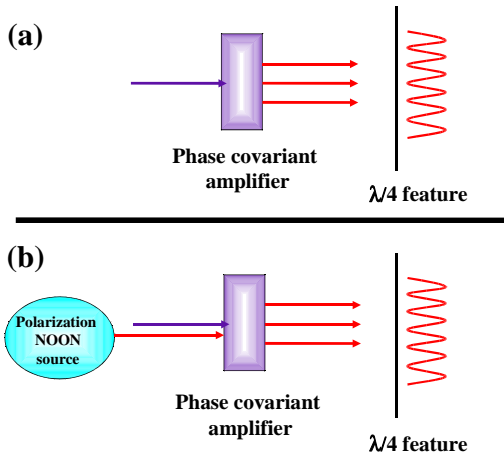


FIG. 1: (a) Unseeded optical parametric amplifier. (b) amplification of a polarization entangled NOON state.

a generic state maintaining the interference pattern of the seed, showing that significant value of the visibilities can be achieved by investigating high-order correlation functions. Finally, the effects of losses are investigated, demonstrating that the amplified field exhibits a higher resilience to losses with respect to a pure NOON state.

II. INTERFEROMETRICAL PATTERN OF THE SEED AND DECOHERENCE

In this section we recall the interferometrical pattern of the injected seed and we study how the state features are affected by losses.

We begin with the polarization entangled NOON state $|\psi^N\rangle_1 = \frac{1}{\sqrt{2}}(|N+\rangle - |N-\rangle)_1$. In this case the N-photon state is entangled in the polarization degree of freedom and belongs to the spatial mode \mathbf{k}_1 . Introducing a phase shift φ between the two orthogonal polarizations, the state reads $|\psi_\varphi^N\rangle_1 = \frac{1}{\sqrt{2}}(|N+\rangle - e^{iN\varphi}|N-\rangle)_1$, where $|p\xi\rangle$ refers to the quantum state with p photons polarized $\vec{\pi}_\xi$. The M-th order correlation function $\mathcal{G}_{seed}^{(M)} = \langle \psi_\varphi^N | \hat{a}_H^\dagger{}^M \hat{a}_H^M | \psi_\varphi^N \rangle$ reads, for $M=N$:

$$\mathcal{G}_{seed}^{(N)} = \frac{N!}{2^N} [1 + (-1)^{N+1} \cos(N\varphi)] \quad (1)$$

while for $M < N$ all the functions do not exhibit any oscillation behaviour and have the expression:

$$\mathcal{G}_{seed}^{(M)} = \frac{N!}{2^M(N-M)!} \quad (2)$$

In order to simulate losses in the transmission path and non unitary detection efficiency, we now introduce a Beam Splitter (BS) of transmittivity η , as shown in Fig.2.

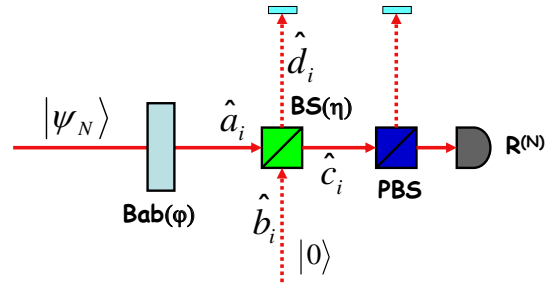


FIG. 2: Decoherence model of the interferometric process. The phase shift in the NOON state $|\psi^N\rangle$ is inserted by a Babinet compensator, while the BS with efficiency η models the decoherence process. The signal is then analyzed in polarization by the PBS and the N photons absorbing device $R^{(N)}$.

The density matrix after the decoherence process, obtained by the insertion of the I/O BS relations and by tracing on the unrevealed reflected mode, becomes:

$$\hat{\rho}_{loss} = \eta^N \hat{\rho}_{NOON} + \sum_{i=0}^{N-1} \binom{N}{i} \eta^i (1-\eta)^{N-i} \hat{\rho}_i \quad (3)$$

where $\hat{\rho}_{NOON} = |\psi_\varphi^N\rangle\langle\psi_\varphi^N|$ is the density matrix of a pure NOON state, and $\hat{\rho}_i = \frac{1}{2} [|i+, 0-\rangle\langle i+, 0-| + |0+, i-\rangle\langle 0+, i-|]$ is the density matrix of a mixed i photons state. Only the first part of this quantum state contributes to the N-th order correlation function, and the successful events rate is reduced by a factor η^N . We finally obtain that the correlation function after losses reads:

$$\mathcal{G}_{loss}^{(N)} = \eta^N \mathcal{G}_{seed}^{(N)} \quad (4)$$

We propose in the following sections to exploit an amplification process in order to improve the robustness to losses of these states without losing their $\frac{\lambda}{N}$ sub-Rayleigh feature.

III. COLLINEAR AMPLIFICATION OF A 2 PHOTON NOON STATE

In this section we study, both theoretically and experimentally, the amplification of a two-photon polarization-entangled NOON state exploiting an optical parametric amplifier working in a collinear configuration. It will be shown that this device cannot be used to amplify a generic N-photon state as its $\frac{\lambda}{2N}$ oscillation pattern is masked by the intrinsic oscillation of the amplification crystal.

A. Theoretical approach

As a first step we consider the generation of a two photon NOON state by spontaneous parametric down conversion in a first crystal over the two polarization mode $\vec{\pi}_+$ and $\vec{\pi}_-$, on the same spatial mode \mathbf{k}_1 . The state generated is $|\psi^2\rangle_1 = \frac{1}{\sqrt{2}}(|2+\rangle - |2-\rangle)_1 = |1H; 1V\rangle_1$, where $|p+; q-\rangle$ stands for the quantum state of p photons polarized $\vec{\pi}_+$ and q photons polarized $\vec{\pi}_-$.

The amplification of the state $|\psi^2\rangle_1$ is realized by injecting the quantum state into a QIOPA acting on the input field \mathbf{k}_1 . The interaction Hamiltonian of the optical parametric amplification $\hat{H}_{coll} = i\chi\hbar\hat{a}_{1H}^\dagger\hat{a}_{1V}^\dagger + h.c.$ acts on the spatial mode \mathbf{k}_1 . The output state over the mode \mathbf{k}_1 is:

$$|\Phi^2\rangle_1 = \frac{1}{C} \sum_{n=0}^{\infty} \Gamma^{n-1} \left(\frac{n}{C^2} - \Gamma^2 \right) |nH; nV\rangle_1 \quad (5)$$

with $C = \cosh g$, $\Gamma = \tanh g$, being g the non-linear gain of the amplification process [17, 18].

The peculiar $\lambda/4$ interference path feature of a two photon NOON state, can be investigated by performing an interferometric measurement on the amplified field. To this end a phase shift θ is introduced, after the amplification stage, in the $\{\vec{\pi}_+, \vec{\pi}_-\}$ basis, corresponding to a rotation of an angle $\theta/2$ in the basis $\{\vec{\pi}_H, \vec{\pi}_V\}$. The state is then analyzed in polarization and detected adopting single photon detectors. The amplified signal can be evaluated by the first order correlation function $\mathcal{G}_{N=2}^{(1)} = {}_1\langle\Phi^2|\hat{c}_1^\dagger\hat{c}_1|\Phi^2\rangle_1$, where $\hat{c}_1^\dagger = (\cos\theta/2\hat{a}_{1H}^\dagger - \sin\theta/2\hat{a}_{1V}^\dagger)$ is the transmitted mode of a polarizing beam splitter (PBS). We find that $\mathcal{G}_{N=2}^{(1)} = 3\bar{n} + 1$, independently of the phase value θ , with $\bar{n} = \sinh^2 g$. The state generated by the amplifier is then investigated through the second order correlation function $\mathcal{G}_{N=2}^{(2)} = {}_1\langle\Phi^2|\hat{c}_1^\dagger\hat{c}_1^\dagger\hat{c}_1\hat{c}_1|\Phi^2\rangle_1$. By tuning the phase shift θ , we find that the expression of the second order correlation function is:

$$\mathcal{G}_{N=2}^{(2)} = 2\bar{n}(4 + 7\bar{n}) + \frac{1}{2}(7\bar{n}^2 + 7\bar{n} + 1)(1 - \cos(2\theta)) \quad (6)$$

The corresponding visibility of the obtained fringe pattern is calculated accordingly to the general definition:

$$\mathcal{V}_N^{(M)} = \frac{\mathcal{G}_N^{(M)}(max) - \mathcal{G}_N^{(M)}(min)}{\mathcal{G}_N^{(M)}(max) + \mathcal{G}_N^{(M)}(min)} \quad (7)$$

where M is the order of the correlation and N is the number of photon of the injected seed. In the case of eq.(6) the visibility reads:

$$\mathcal{V}_{N=2}^{(2)} = \frac{7\bar{n}^2 + 7\bar{n} + 1}{35\bar{n}^2 + 23\bar{n} + 1} \quad (8)$$

We observe that a non-vanishing visibility is found for any value of g : $\mathcal{V}_{N=2}^{(2)}(g \rightarrow \infty) = \frac{1}{5}$. The fringe pattern

exhibits a dependence on 2θ and hence a period equal to $\frac{\lambda}{2}$. This feature can be exploited to carry out interferometry with sub-Rayleigh resolution, i.e., with fringe period lower than λ , in a higher flux regime compared to the two photon configurations. The interest in amplifying a NOON state belongs to the trend of visibility as a function of the number of generated photons. Recently, as said, it has been demonstrated [16] that the output field of a collinear parametric amplifier working in spontaneous emission regime shows a $\lambda/4$ feature. There an unseeded optical parametric amplifier working in collinear regime was pumped by an UV beam. The output radiation, after a phase shifter, was analyzed in polarization. The fringe pattern visibility in that case was $\mathcal{V}_{N=0}^{(2)} = \frac{\bar{n}+1}{5\bar{n}+1}$. The asymptotical values of visibilities in the two regimes, spontaneous and stimulated, are equal; on the contrary for an intermediate number of generated photons the visibility in the amplified regime is higher than that in the spontaneous one as shown in Fig. 3-(a). Hence, the injection of a seed with theoretical visibility equal to 1 leads to an advantage in the visibility for the amplified field with respect to the case of spontaneous emission. We note that the same average number of photons in the two regimes is achieved for different values of the gain. In the spontaneous regime the average photons number generated by the amplifier is $\langle\hat{n}\rangle_{sp} = 2 \sinh^2 g$, on the contrary, for the same gain value, in the stimulated regime we have: $\langle\hat{n}\rangle_{stim} = 2 + 6 \sinh^2 g$. For a value

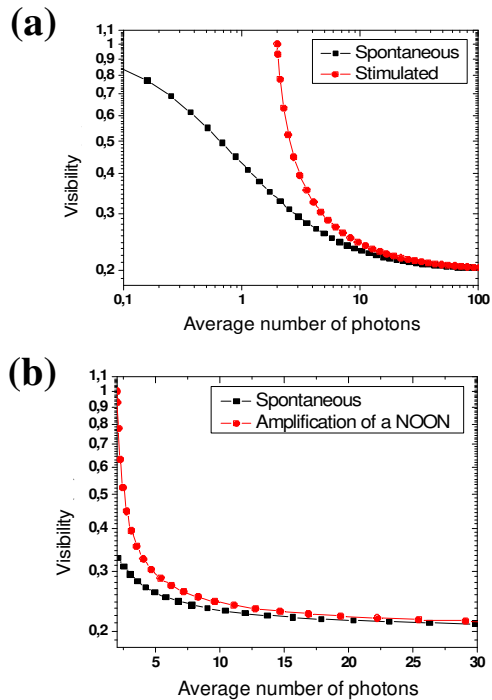


FIG. 3: Theoretical trend of the visibility in function of the number of photons generated by the amplification in the two cases: spontaneous and stimulated.

of the gain $g = 0$ the number of photons in the stimulated case is $\langle \hat{n} \rangle_{stim} = 2$, unlike the spontaneous case in which $\langle \hat{n} \rangle_{sp} = 0$. In both cases the value of visibility tends to 1 for $g \rightarrow 0$. By analyzing the trends of visibilities in Fig.3-(b) we see that the advantage of amplifying a NOON state holds until $\langle \hat{n} \rangle \simeq 30$.

An enhancement of the fringe pattern can be obtained by evaluating the M-th order visibility $\mathcal{V}_{N=2}^{(M)}$, with $M > 2$, corresponding to the M-th order correlation function at time t : $\mathcal{G}_{N=2}^{(M)} = {}_1\langle \psi^2 | [\hat{c}_1^\dagger(t)]^M [\hat{c}_1(t)]^M | \psi^2 \rangle_1$. This calculation have been performed in the Heisenberg picture, where the field operator $\hat{c}_1^\dagger(t)$ is the time evolution of the analyzed field \hat{c}_1^\dagger solving the Heisenberg equations for the collinear OPA. We calculated the first 6 orders correlation functions, obtaining the following visibilities:

$$\mathcal{V}_{N=2}^{(2)} = \frac{1 + 7\bar{n} + 7\bar{n}^2}{1 + 25\bar{n} + 35\bar{n}^2} \quad (9)$$

$$\mathcal{V}_{N=2}^{(3)} = \frac{12 + 48\bar{n} + 39\bar{n}^2}{12 + 84\bar{n} + 91\bar{n}^2} \quad (10)$$

$$\mathcal{V}_{N=2}^{(4)} = \frac{12 + 291\bar{n} + 822\bar{n}^2 + 567\bar{n}^3}{12 + 291\bar{n} + 1078\bar{n}^2 + 903\bar{n}^3} \quad (11)$$

$$\mathcal{V}_{N=2}^{(5)} = \frac{135 + 1315\bar{n} + 2845\bar{n}^2 + 1705\bar{n}^3}{135 + 1315\bar{n} + 3245\bar{n}^2 + 2201\bar{n}^3} \quad (12)$$

$$\mathcal{V}_{N=2}^{(6)} = \frac{45 + 1745\bar{n} + 10080\bar{n}^2 + 17507\bar{n}^3 + 9245\bar{n}^4}{45 + 1745\bar{n} + 10080\bar{n}^2 + 18657\bar{n}^3 + 10621\bar{n}^4} \quad (13)$$

The theoretical plots of the visibilities are reported in Fig.4. We observe that an increasing trend is obtained by exploiting correlation functions with higher order M . This means that analyzing a higher order absorption process the contrast of the fringe pattern is enhanced. This feature was also predicted in the spontaneous emission regime in [21], and experimentally observed in [16].

B. Experimental verification

The previous theoretical results have been experimentally verified adopting an injected high-gain optical parametric amplifier. The experimental setup is sketched in Fig 5.

The excitation source was a Ti:Sa Coherent MIRA mode-locked laser amplified by a Ti:Sa regenerative REGA device operating with pulse duration 180fs at a repetition rate of 250kHz. The output beam, frequency-doubled by second harmonic generation, provided the excitation beam of UV wavelength (wl) $\lambda_P = 397.5\text{nm}$ and power 750mW. The UV beam was split in two beams through a $\lambda/2$ waveplate and a polarizing beam splitter (PBS) and excited two BBO (β -barium borate) NL crystals cut for type II phase-matching. The pump power of beam \mathbf{k}_P was set in order to have a negligible probability to generate three couples of photons ($< 10\%$). Let us describe how the 2-photon state $|\psi^2\rangle_1 = 2^{-1/2}(|2+\rangle - |2-\rangle)_1 = |1H; 1V\rangle_1$ was conditionally generated on mode \mathbf{k}_1 . We adopted the scheme

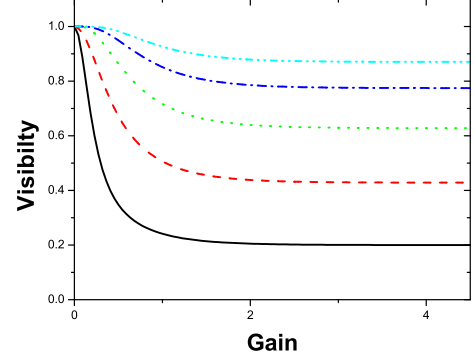


FIG. 4: Plot of the visibilities $\mathcal{V}_{N=2}^{(M)}$ with $2 \leq M \leq 6$ for the collinear QIOPA in stimulated emission with the injection of a 2-photon NOON state as a function of the nonlinear gain g . Straight line corresponds to $\mathcal{V}_{N=2}^{(2)}$, dashed line to $\mathcal{V}_{N=2}^{(3)}$, dotted line to $\mathcal{V}_{N=2}^{(4)}$, dash-dotted line do $\mathcal{V}_{N=2}^{(5)}$ and short dash-dotted line to $\mathcal{V}_{N=2}^{(6)}$.

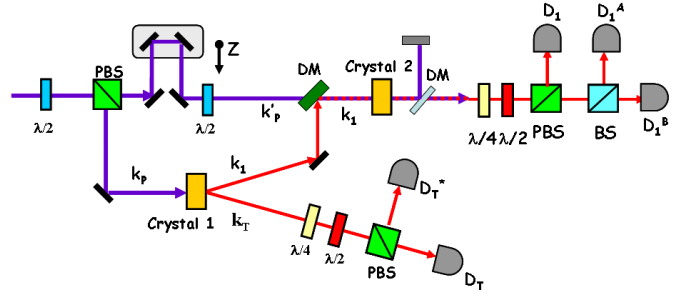


FIG. 5: Experimental scheme adopted to amplify a 2-photon state. By measuring coincidences between detector $\{D_T, D_T^*\}$ on spatial mode \mathbf{k}_T , the state on spatial mode \mathbf{k}_1 is prepared in the two-photon NOON state $|\psi^2\rangle_1$. The rate of the trigger signal was around 10^4Hz and the rate of coincidences between (D_T, D_T^*) was around 400Hz .

demonstrated by Eisenberg et al [19]: Crystal 1, excited by the beam \mathbf{k}_P , is the spontaneous parametric down-conversion (SPDC) source of entangled photons of wavelength $\lambda = 2\lambda_P$, emitted over the two output modes \mathbf{k}_i ($i = 1, T$), where T stands for the trigger mode, in the state $|\Psi_2^-\rangle_{1T} = \frac{1}{\sqrt{3}}(|2H\rangle_1|2V\rangle_T - |1H; 1V\rangle_1|1H; 1V\rangle_T + |2V\rangle_1|2H\rangle_T)$. The two photons associated to mode \mathbf{k}_T were coupled into a single mode fiber and excited two single photon counting module (SPCM) $\{D_T, D_T^*\}$. The state $|1H; 1V\rangle_T$ was detected on mode \mathbf{k}_T by measuring the coincidences between detectors $\{D_T, D_T^*\}$ in the $\{\vec{\pi}_H, \vec{\pi}_V\}$ polarization basis on mode \mathbf{k}_T leading to the conditional preparation of the state $|1H; 1V\rangle_1$ on mode \mathbf{k}_1 .

The amplification of the injected 2-photon state was achieved by superimposing the pump beam on mode \mathbf{k}'_1 and the field on mode \mathbf{k}_1 on crystal II exploiting a

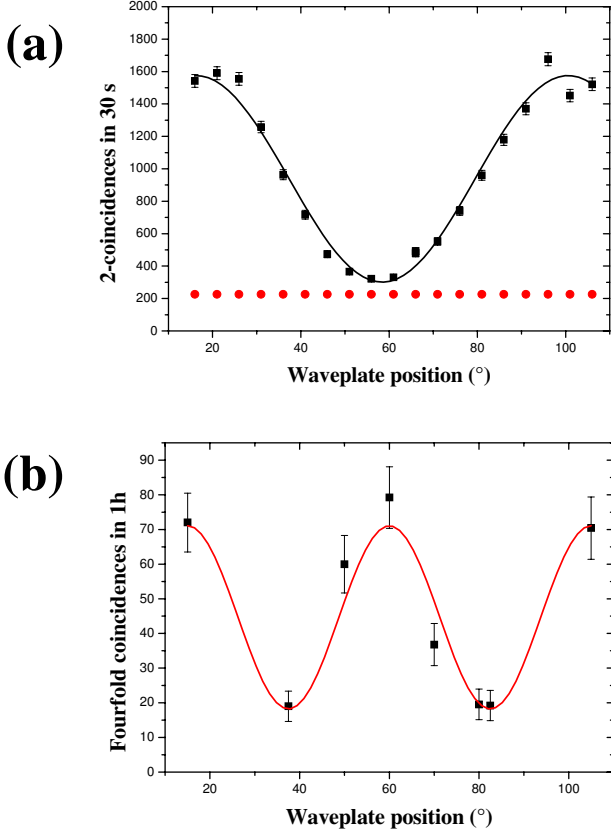


FIG. 6: (a) Fringe pattern of the two-fold-coincidences between detectors $\{D_1^B, D_T\}$ (b) Fringe pattern of the four-fold-coincidences between detectors $\{D_1, D_1^B, D_T, D_T^*\}$.

dichroic mirror (DM) with high reflectivity at λ and high transmittivity at λ_p . The output radiation was then analyzed through a polarizing beam splitter (PBS) and detected adopting single photon detectors SPCM-AQR14 (D_1^A, D_1^B, D_1).

In order to characterize the state produced by the first crystal, a measurement of the second order correlation function of the injected field, without the contribution of the UV pump beam on crystal 2, was carried out. The typical $\lambda/4$ fringe pattern was measured by the fourfold coincidences between detectors $\{D_1, D_1^B, D_T, D_T^*\}$, through evaluation of the second order correlation function $G_{seed}^{(2)} = {}_1\langle \psi^2 | \hat{c}_1^\dagger \hat{c}_2^\dagger \hat{c}_2 \hat{c}_1 | \psi^2 \rangle_1$, where $\hat{c}_2^\dagger = (\sin \theta / 2 \hat{a}_{1H}^\dagger + \cos \theta / 2 \hat{a}_{1V}^\dagger) = \hat{c}_{1\perp}^\dagger$. The obtained visibility $\mathcal{V}_{seed}^{(2)} = (63 \pm 4)\%$ is lower than the expected one, due to the experimental imperfections and to the emission of higher number of photons by the first crystal. In Fig.6 we report the oscillation of the injected field with (Fig.6-(b)) and without (Fig.6-(a)) the conditional generation of the two photon NOON state by the first crystal. As shown, the two-fold coincidences present a λ period and the $\lambda/4$ feature is displayed only by the fourfold coincidences Fig.6-(b).

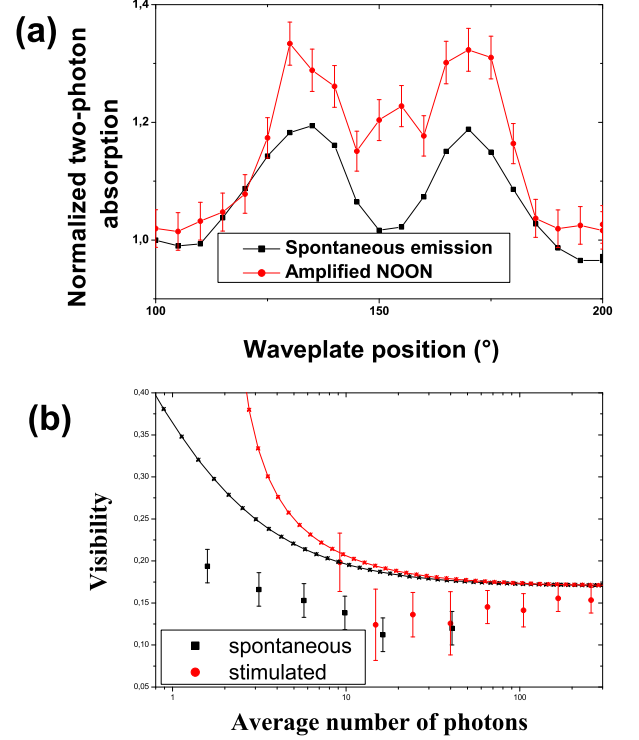


FIG. 7: (a) Oscillation fringe patterns in the stimulated and spontaneous regimes. The unbalanced minima are due to a different coupling of the $\vec{\pi}_H$ and $\vec{\pi}_V$ polarized signals with the single mode fiber. (b) Visibility value $\mathcal{V}_{N=2}^{(2)}$ as a function of NL gain g in the spontaneous (triangular dots) and stimulated case (circular dots). Experimental (points) and theoretical trend in the stimulated regime (curve) are shown. The theoretical curve used are: $V_{sp} = 0.85 \mathcal{V}_{N=0}^{(2)}$ and $V_{stim} = 0.85 \mathcal{V}_{N=2}^{(2)}$. The factor 0.85 has been inserted to consider experimental imperfections. The curves are parametric plotted as a function of the respective number of generated photons, which are $\langle \hat{n} \rangle_{sp} = 2 \sinh^2 g$ and $\langle \hat{n} \rangle_{stim} = 2 + 6 \sinh^2 g$. Data in the spontaneous regime refer to work [16].

We characterized then the state generated by the second crystal by evaluating the correlation function $\mathcal{G}^{(2)}$ in the spontaneous, by detecting coincidences between detectors $\{D_1^A, D_1^B, D_T\}$, and stimulated regime, by detecting coincidences between detectors $\{D_1^A, D_1^B, D_T, D_T^*\}$, for a value of the NL gain $g = 2$ [19, 20]. We observed that the $\lambda/2$ period has been preserved by the amplification process Fig.7-(a). The minima, at 105° and 150° , correspond to polarizations $\vec{\pi}_H$ and $\vec{\pi}_V$. The unbalancing between the two values of the absorption rate is due to a different coupling of the two orthogonal linear polarizations with the single mode fiber. This effect is related with the distinguishability, i.e spectral difference, between the ordinary and extraordinary wave vectors cones generated by the second crystal during the amplification process. The visibility has been evaluated through the definition

$\mathcal{V} = \frac{C_{max}^{(4)} - C_{min}^{(4)}}{C_{max}^{(4)} + C_{min}^{(4)}}$, where $C^{(4)}$ is the value of the fourfold coincidences. In particular, only a portion of the global fringe pattern of Fig.7 has been used to calculate the visibility. Only the maximum and the adjacent minimum which exhibit the higher contrast were considered, as a $\frac{\pi}{N}$ interval of the fringe pattern, showing a $\frac{\lambda}{2N}$ resolution, is necessary for quantum lithographic applications. By the same measurement we observe the fringe patterns for different gain values by increasing the UV pump beam. We report in Fig. 7-(b) the trend of visibility as a function of the number of photons generated: the spontaneous visibilities have been taken from [16]. The experimental data are compared with theoretical predictions in both regimes: spontaneous and stimulated. The theoretical trends have been scaled by a factor 0.85, that was the asymptotical visibility obtained in the spontaneous case in [16], due to experimental imperfections. In the amplified case the experimental asymptotical visibility is affected both by experimental imperfections and by the emission of higher number of photons by the first crystal. We observe that both the data points for increasing gain values move away from the theoretical trends. This can be due to a partial multimode operation of the parametric amplifier [22]. We conclude that the value of visibility in the two regime is almost the same, but an enhancement of the signal in the stimulated case has been observed.

Indeed the probability of observing a sub-Rayleigh phenomenon is proportional to the second order correlation function $\mathcal{G}^{(2)}$ in both regimes. By the theory, the stimulated signal is seven time higher than the spontaneous one: $\frac{\mathcal{G}_{N=2}^{(2)}}{\mathcal{G}_{N=0}^{(2)}} = 7$. Experimentally we can evaluate this ratio by the following method: the probability of detecting coincidences in the spontaneous case is $P_{sp} = \frac{C^{(2)}}{R}$, where $C^{(2)}$ are coincidences between detectors $\{D_1^A, D_1^B\}$ and R is the repetition rate. In the stimulated case it reads : $P_{stim} = \frac{C^{(4)}}{\Xi}$, where $C^{(4)}$ are coincidences between detectors $\{D_T, D_T^*, D_1^A, D_1^B\}$, and Ξ are coincidences between detectors $\{D_T, D_T^*\}$ on trigger mode, that is the rate of injection of the two photon NOON state in the QIOPA per second. Hence the ratio between the two probabilities is : $\frac{P_{stim}}{P_{sp}} = (6.21 \pm 0.8)$.

C. Amplification of $N > 2$ states

As last step, we investigate the amplification of N -photon NOON states with $N > 2$ with the same device. The injection of a 3-photon state $|\psi^3\rangle_1 = 2^{-1/2}(|3+\rangle - |3-\rangle)_1$ leads to an amplified wave function of the form:

$$|\Phi^3\rangle = \frac{1}{\sqrt{12}C^4} \sum_{i,j=0}^{\infty} \frac{\left(\frac{\Gamma}{2}\right)^i \left(-\frac{\Gamma}{2}\right)^j}{i!j!} \left\{ \sqrt{(2i+3)!2j!} |(2i+3)+, (2j)-\rangle - \sqrt{2i!(2j+3)!} |(2i)+, (2j+3)-\rangle \right\} + \frac{\Gamma\sqrt{3}}{2C^2} \sum_{i,j=0}^{\infty} \frac{\left(\frac{\Gamma}{2}\right)^i \left(-\frac{\Gamma}{2}\right)^j}{i!j!} \left\{ \sqrt{(2i+1)!2j!} |(2i+1)+, (2j)-\rangle + \sqrt{2i!(2j+1)!} |(2i)+, (2j+1)-\rangle \right\} \quad (14)$$

Let us analyze the expression of the quantum state in equation (14). We expect the third order correlation function to have oscillation in all the three harmonics θ , 2θ and 3θ . In fact, the first part of the wave function contains the sum of quantum states of the form $|2i+3, 2j\rangle - |2i, 2j+3\rangle$. These are analogous to 3 photons NOON states with a common background $2i, 2j$ generated by the crystal, thus leading to a $\frac{\lambda}{3}$ period. The same argument holds for the second part of eq.(14), as the unbalancement of only 1 photon determines a λ period. We finally expect the presence of a $\frac{\lambda}{2}$ period due to the couple emission of photons by the crystal. Explicit calculation of the third order correlation function gives the result:

$$\mathcal{G}_{N=3}^{(3)} = a(\bar{n}) + b(\bar{n}) \cos(\theta) + c(\bar{n}) \cos(2\theta) + d(\bar{n}) \cos(3\theta) \quad (15)$$

where $a(\bar{n}) = 6 + 342\bar{n} + 1782\bar{n}^2 + 1824\bar{n}^3$ and $c(\bar{n}) = \frac{1}{2} [81\bar{n} + 369\bar{n}^2 + 288\bar{n}^3]$ are third degree polynomial in \bar{n} , while $b(\bar{n}) = \frac{3}{2} [3\bar{n}^2 + 3\bar{n} + 1]$ and $d(\bar{n}) = -\frac{27}{2} [\bar{n} + \bar{n}^2]$ are second degree polynomial in \bar{n} . We find, as said, the presence of oscillating terms at the three fundamental harmonics in θ , 2θ and 3θ . The term in 2θ is dominant for high gain values, and the intrinsic oscillation of the crystal with period $\frac{\lambda}{2}$ suppresses the amplitude of the oscillations with $\frac{\lambda}{3}$ period. Hence this apparatus based on the collinear QIOPA device cannot be used for the amplification of a generic state, as the interference pattern of the seed is masked during the amplification process.

Hence in order to preserve the $\frac{\lambda}{2N}$ phase oscillation after the amplification process, a different amplifier device, not containing an intrinsic phase oscillation, has to be employed.

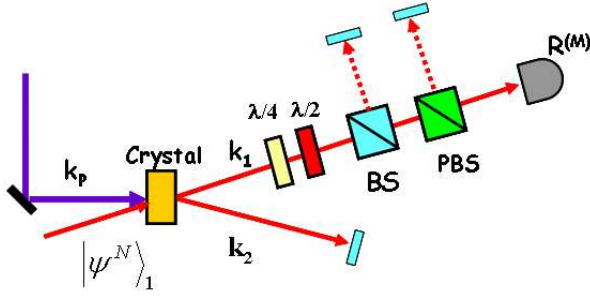


FIG. 8: Experimental setup for the amplification of a NOON state by a non-collinear amplifier, implemented by a type-II cut BBO crystal in non collinear configuration. The state $|\psi^N\rangle_1$ is injected into the input mode \mathbf{k}_1 . The BS is inserted in order to simulate losses.

IV. NON COLLINEAR AMPLIFIER

In this section we study the amplification of NOON states exploiting an Optical Parametric Amplifier working in a non-collinear configuration. The interaction Hamiltonian of this device is [17]:

$$\hat{\mathcal{H}}_{int} = i\hbar\chi \left(\hat{a}_{1\pi}^\dagger \hat{a}_{2\pi}^\dagger - \hat{a}_{1\pi_\perp}^\dagger \hat{a}_{2\pi_\perp}^\dagger \right) + \text{h.c.} \quad (16)$$

where π, π_\perp stand for any two orthogonal polarizations, as this configuration is invariant under $SU(2)$ rotations. The proposed scheme is shown in Fig.8.

After the preparation of the seed, the state is injected on mode \mathbf{k}_1 in the amplifier together with the pump beam \mathbf{k}_p to obtain the amplification process. A phase shift θ is then introduced between the two polarization $\vec{\pi}_+, \vec{\pi}_-$ and the M -th order absorption process is performed in $R^{(M)}$. An unbalanced BS with transmittivity η will be subsequently introduced in Sec.IV D to simulate losses and non unitary efficiency of detection. This scheme corresponds to evaluating the M -th order correlation defined by the operator $\hat{G}^{(M)} = [\hat{c}_1^\dagger(t)]^M [\hat{c}_1(t)]^M$, where \hat{c}_1^\dagger is the creation operator associated to the revealed mode corresponding to the Heisenberg evolution of the field operator \hat{a}_{1H} :

$$\hat{c}_1^\dagger(t) = \frac{1}{\sqrt{2}} \left[\hat{a}_{1+}^\dagger(t) - e^{i\theta} \hat{a}_{1-}^\dagger(t) \right] \quad (17)$$

The time evolution of the field operators in the crystal is derived from the interaction Hamiltonian of the non-collinear OPA (16). The Heisenberg equations gives:

$$\hat{a}_{1+}^\dagger(t) = \hat{a}_{1+}^\dagger \cosh(g) + \hat{a}_{2-} \sinh(g) \quad (18)$$

$$\hat{a}_{1-}^\dagger(t) = \hat{a}_{1-}^\dagger \cosh(g) + \hat{a}_{2+} \sinh(g) \quad (19)$$

where $g = \chi t_{int}$ is the non-linear gain of the process.

A. Spontaneous emission

Let us study the interferometrical feature of this device in the spontaneous emission case. It will be shown that the spontaneous emitted field does not show any oscillation patterns for any orders of correlation.

The unitary time evolution operator in the interaction picture for the non-collinear OPA can be written in the form [17]:

$$\hat{U} = e^{\Gamma(\hat{a}_{1+}^\dagger \hat{a}_{2-}^\dagger - \hat{a}_{1-}^\dagger \hat{a}_{2+}^\dagger)} e^{-\ln C(1 + \hat{n}_{1+} + \hat{n}_{1-} + \hat{n}_{2+} + \hat{n}_{2-})} e^{\Gamma(\hat{a}_{1-} \hat{a}_{2+} - \hat{a}_{1+} \hat{a}_{2-})} \quad (20)$$

where $C = \cosh(g)$ and $\Gamma = \tanh(g)$. Applying this operator to the input vacuum state we obtain:

$$|\Phi\rangle = \frac{1}{C} \sum_{n=0}^{\infty} \Gamma^n \sum_{m=0}^n |(n-m)_+, m_-\rangle_1 |m_+, (n-m)_-\rangle_2 \quad (21)$$

The M -th order correlation function, calculated in the Heisenberg picture shows that there is no oscillation pattern in the spontaneous radiation. Let us ignore for now the effects of losses, and evaluate $\mathcal{G}_0^{(M)} = \langle 0 | \hat{G}^{(M)} | 0 \rangle$. The M -th order correlation operator reads:

$$\hat{G}^{(M)} = \frac{1}{2^M} \left[\hat{a}_{1+}^\dagger C + \hat{a}_{2-} S - e^{i\theta} \hat{a}_{1-}^\dagger C - e^{i\theta} \hat{a}_{2+} S \right]^M \times \left[\hat{a}_{1+} C + \hat{a}_{2-}^\dagger S - e^{-i\theta} \hat{a}_{1-} C - e^{-i\theta} \hat{a}_{2+}^\dagger S \right]^M \quad (22)$$

where $S = \sinh(g)$. This operator can be written, using the multinomial expansion, as:

$$\hat{G}^{(M)} = \frac{1}{2^M} \left(\sum_{i,j,k} g_{ijk} (\hat{a}_{1+}^\dagger)^{M-i-j-k} (\hat{a}_{2-})^i (\hat{a}_{1-}^\dagger)^j (\hat{a}_{2+})^k \right) \times \left(\sum_{l,m,n} g_{lmn}^* (\hat{a}_{1+})^{M-i-j-k} (\hat{a}_{2-})^i (\hat{a}_{1-}^\dagger)^j (\hat{a}_{2+})^k \right) \quad (23)$$

where:

$$g_{ijk} = \left(\frac{1}{\sqrt{2}} \right)^M \binom{M}{i, j, k} (-1)^{j+k} (e^{i\theta})^{j+k} C^{M-i-k} S^{i+k} \quad (24)$$

and the sums are extended as $\sum_{i=0}^M \sum_{j=0}^{M-i} \sum_{k=0}^{M-i-j}$. The average of $\hat{G}^{(M)}$ on the vacuum input state gives:

$$\mathcal{G}_0^{(M)} = M! S^{2M} \quad (25)$$

This expression is independent on the phase for any order of the correlation. Thus, no intrinsic phase oscillation pattern is present in the radiation emitted in the spontaneous regime by the non collinear OPA, as expected from the form of the interaction Hamiltonian of eq.(16).

B. Amplified NOON quantum state

First we calculate the quantum state in the interaction picture. The amplified field is obtained, with a procedure

$$|\Phi^N\rangle = \frac{1}{\sqrt{2}\sqrt{N!}C^{N+1}} \sum_{n=0}^{\infty} \Gamma^n \sum_{m=0}^n (-1)^m \times \left[\sqrt{\frac{(n-m+N)!}{(n-m)!}} |(n-m+N)+, m-\rangle_1 - \sqrt{\frac{(m+N)!}{m!}} |(n-m)+, (m+N)-\rangle_1 \right] |m+, (n-m)-\rangle_2 \quad (26)$$

Let us analyze the expression (26): the N-photons in excess on the two polarization modes with respect to the spontaneous emission case of eq.(21) are responsible for the $\frac{\lambda}{2N}$ fringe pattern. Hence the original N photons in the injected state are added to a background field emitted by the crystal.

C. M-th order correlation function

We now calculate the generic M-th order correlation function with the injection of a NOON state defined by the average $\mathcal{G}_N^{(M)} = {}_{c_1} \langle \psi^N | \hat{G}^{(M)} | \psi^N \rangle_{c_1}$. It will be shown that the original features of the injected seed will be maintained. It will be explicitly demonstrated that the correlation functions of order $M < N$ do not have any oscillation patterns, while the ones with $M \geq N$ exhibit sub-Rayleigh $\frac{\lambda}{2N}$ feature. The value of the correlation functions can be calculated in the Heisenberg picture analogously to the spontaneous case of Sec.IV A. We obtain the following expression for $\mathcal{G}_N^{(M)}$:

$$\begin{aligned} \mathcal{G}_N^{(M)} = & \frac{M!}{2^M} \left\{ \sum_{i=0}^{M-N} \sum_{j=0}^N C^{2j} S^{2(M-j)} \binom{N}{j} \binom{M}{i, j} + \right. \\ & + \sum_{i=M-N+1}^M \sum_{j=0}^{M-i} C^{2j} S^{2(M-j)} \binom{N}{j} \binom{M}{i, j} + \\ & \left. - (-1)^M C^{2N} S^{2(M-N)} \left[\sum_{i=0}^{M-N} \binom{M}{i, N} \right] \cos(N\theta) \right\} \quad (27) \end{aligned}$$

for $M \geq N$, while for $M < N$ we obtain:

$$\mathcal{G}_N^{(M)} = \frac{M!}{2^M} \sum_{i=0}^M \sum_{j=0}^{M-i} C^{2j} S^{2(M-j)} \binom{M}{i, j} \binom{N}{j} \quad (28)$$

The form of eq.(27) explicitly shows the $\frac{\lambda}{N}$ period

completely analogous to the spontaneous emission case calculated in Sec.IV A, by applying the operator (20) to the injected state: $|\Phi^N\rangle = \hat{U}|\psi^N\rangle_1$. The output state reads:

of the emitted radiation, as only constant or oscillating terms in $N\theta$ are present.

D. Losses and decoherence effects

We are now interested in studying the effects of losses and of non unitary efficiency of detection on the amplified field. We introduce an unbalanced BS of transmittivity η in spatial mode \mathbf{k}_1 (Fig. 8). The two BS input modes are labelled by $\hat{b}_1^\dagger(t)$ and $\hat{c}_1^\dagger(t)$, where the second one is the OPA output mode and the first one is the vacuum input lossy channel. The revealed output mode corresponds to the field operator:

$$\hat{d}_1^\dagger(t) = \sqrt{\eta} \hat{c}_1^\dagger(t) + \iota \sqrt{1-\eta} \hat{b}_1^\dagger(t) \quad (29)$$

where the BS I/O relations have been used. The M-th order correlation function $\tilde{\mathcal{G}}_N^{(M)} = {}_{b_1} \langle 0 | {}_{c_1} \langle \psi^N | \{ [\hat{d}_1^\dagger(t)]^M [\hat{d}_1(t)]^M \} | \psi^N \rangle_{c_1} | 0 \rangle_{b_1}$ reads:

$$\begin{aligned} \tilde{\mathcal{G}}_N^{(M)} = & \sum_{i,j=0}^M (\sqrt{\eta})^{i+j} (\iota \sqrt{1-\eta})^{2M-i-j} (-1)^{M-j} \times \\ & {}_{b_1} \langle 0 | {}_{c_1} \langle \psi^N | \{ [\hat{c}_1^\dagger(t)]^i [\hat{b}_1^\dagger(t)]^{M-i} [\hat{c}_1(t)]^j [\hat{b}_1(t)]^{M-j} \} | \psi^N \rangle_{c_1} | 0 \rangle_{b_1} \quad (30) \end{aligned}$$

The input vacuum field on mode \hat{b}_1 imposes the constraints $i = M$ and $j = M$ when we evaluate the average. The correlation function $\tilde{\mathcal{G}}_N^{(M)}$ then reads:

$$\tilde{\mathcal{G}}_N^{(M)} = \eta^M {}_{c_1} \langle \psi^N | [\hat{c}_1^\dagger(t)]^M [\hat{c}_1(t)]^M | \psi^N \rangle_{c_1} = \eta^M \mathcal{G}_N^{(M)} \quad (31)$$

Hence, the presence of losses and of the non unitary efficiency of detection do not change the oscillation pattern of the amplified field, but only reduce the efficiency of the process by a factor η^N . The main difference between the pure NOON state and the amplified field is in their resilience to losses. For the injected state, as explained in

Sec.II, the loss of just a single photon cancels the $\frac{\lambda}{N}$ behaviour of the field and only a fraction η^N contributes to the successful events rate. On the contrary, for the amplified field the non-linear gain of the process can be chosen so that $\eta^M \bar{n} \gg 1$. In this condition, the large majority of the pulses give contribution to the M-th order correlation and the successful events rate is substantially not reduced.

E. Asymptotical visibilities

Knowing the correlation function, we can calculate the visibilities associated to this M-photon absorption processes. We can see by the form of eq.(31) that the visibility associated to the M-th order correlation function is not affected by losses and by non unitary detection efficiency. Restricting our attentions to the asymptotical visibilities, corresponding to $g \rightarrow \infty$ and hence to an ideal infinite number of photons in the emitted field, we obtain for a NOON state with $N=2,3,4$ the following expressions:

$$\tilde{V}_{N=2}^{(M)}(\bar{n} \rightarrow \infty) = \frac{M^2 - M}{M^2 + 7M + 8} \quad (32)$$

$$\tilde{V}_{N=3}^{(M)}(\bar{n} \rightarrow \infty) = \frac{M^3 - 3M^2 + 2M}{M^3 + 15M^2 + 56M + 48} \quad (33)$$

$$\tilde{V}_{N=4}^{(M)}(\bar{n} \rightarrow \infty) = \frac{M^4 - 6M^3 + 11M^2 - 6M}{M^4 + 26M^3 + 203M^2 + 538M + 384} \quad (34)$$

The plot of these three functions are reported in Fig.9. We observe that the values of the visibilities grow with

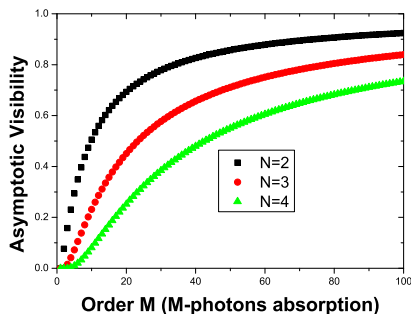


FIG. 9: Plot of the asymptotic ($g \rightarrow \infty$ and $\bar{n} \rightarrow \infty$) M-th order correlation function as a function of the order M in three cases. The square data corresponds to the injection of a 2-photons state, the circular data to a 3-photons state and the triangular data to a 4-photons state.

the order of correlation M and decrease as the number of photons of the injected states increases. This is due to the characteristic of the N-photon NOON seed, which implies an increase of both the minimum and the maximum of the fringe pattern proportional to the number of photons N.

V. CONCLUSION

In this paper we investigated the amplification of a two photons NOON state using two different scheme both based on the process of optical parametric amplification. In Sec.II we reviewed how this kind of quantum states are extremely sensitive to losses. In Sec.III we propose to use a collinear optical parametric parametric amplifier to amplify a 2-photon entangled state, maintaining in the output field the $\frac{\lambda}{4}$ pattern of the injected seed. We analyzed the problem theoretically and experimentally, comparing the amplified with the spontaneous emission regime analyzed in [16]. We found experimentally that the two regimes have comparable visibilities, while the advantage of the stimulated case is a significant increase of the number of photons in the emitted radiation. We then showed that this device, due to the intrinsic $\frac{\lambda}{4}$ oscillation of the radiation emitted by the crystal, cannot be used to amplify a generic N photon states. We then propose in Sec.IV to use a non-collinear optical parametric amplifier to amplify a generic NOON state. We showed that the oscillation period of the seed is maintained during the amplification process and the visibility reaches an asymptotical unitary value when the M-th order correlation function with sufficiently high value of M is analyzed. Furthermore, we showed that the amplified field exhibits a high resilience to losses with respect to the extreme sensitivity of the NOON states.

We acknowledge useful and stimulating discussions with Jonathan P. Dowling. This work was supported by the PRIN 2005 of MIUR and Progetto Innesco 2006 (CNISM).

-
- [1] A.N. Boto, et al., Phys. Rev. Lett. **85**, 2733 (2000); P. Kok, et al., Phys. Rev. A **63**, 063407 (2001).
 [2] M.J. Holland, Phys. Rev. Lett. **71**, 1355 (1993); J.P. Dowling, Phys. Rev. A **57**, 4736 (1998).
 [3] V. Giovannetti, et al., Phys. Rev. Lett. **96**, 010401 (2006).
 [4] M. D'Angelo, et al., Phys. Rev. Lett. **87**, 013602 (2001).
 [5] K.T. Kapale, et al., quant-ph/0612196; H. Cable, et

- al., quant-ph/0704.0678; A.E.B. Nielsen, et al., quant-ph/0704.0397.
 [6] K. Edamatsu, et al., Phys. Rev. Lett. **89**, 213601 (2002).
 [7] M.W. Mitchell, et al., Nature (London) **429**, 161 (2004).
 [8] P. Walther, et al., Nature (London) **429**, 158 (2004); T. Nagata, et al., Science **316**, 726 (2007).
 [9] H.S. Eisenberg, et al., Phys. Rev. Lett. **94**, 090502 (2005).

- [10] H.F. Hofmann, et al., Phys. Rev. A **76**, 031806 (R) (2007).
- [11] H. Cable et al., Phys. Rev. Lett. **99**, 163604 (2007)
- [12] F. De Martini, Phys. Rev. Lett. **81**, 2842 (1998).
- [13] F. De Martini et al., Nature (London) **419**, 815-818 (2002)
- [14] F. De Martini et al., Phys. Rev. Lett. **95**, 240401 (2005)
- [15] T. De Angelis et al., Phys. Rev. Lett. **99**, 193601 (2007)
- [16] F. Sciarrino, et al., Phys. Rev. A **77**, 012324 (2008).
- [17] F. De Martini and F. Sciarrino, Progress in Quantum Electronics **29**, 165 (2005).
- [18] F. De Martini, G. Di Giuseppe, and S. Padua, Phys. Rev. Lett. **87**, 150401 (2001).
- [19] H.S. Eisenberg, *et al.*, Phys. Rev. Lett. **93**, 193901 (2004).
- [20] M. Caminati, *et al.*, Phys. Rev. A **73**, 032312 (2006).
- [21] G. S. Agarwal et al., J. Opt. Soc. Am. B **24**, 270 (2007); E. M. Nagasako et al, Phys. Rev. A **64**, 043802 (2001)
- [22] S. Thanvanthri *et al.*, Phys. Rev. A **70**, 063811 (2004).